Three-dimensional finite element analysis of vortex-induced vibration in deepwater steel catenary risers with large deformation

Zhenhua Li[1], Carlos E. Silva[2], José L. D. Alves[2], Leandro Gazoni[2], Yangye He[4], Jian Su[1]

[1]*Nuclear Engineering Department,COPPE, Universidade Federal do Rio de Janeiro*
Centro de Tecnologia, Bloco I, Sala 214, 21941-909, Rio de Janeiro, Brazil
zhenhua.li@lasme.coppe.ufrj.br, sujian@coppe.ufrj.br
[2]*Laboratory for Computational Methods in Engineering*
Federal University of Rio de Janeiro, R. Paulo Emídio Barbosa, 485, 21941-853, Rio de Janeiro, Brazil
kadu@promecgroup.com, gazoni@promecgroup.com, jalves@lamce.coppe.ufrj.br
[3]*China University of Petroleum-Beijing, 102249, Beijing, China*
yangyehe@cup.edu.cn

Abstract. A numerical study on the cross-flow (CF) vortex-induced vibration (VIV) of a steel catenary riser (SCR) under uniform flow load in three-dimensional large displacement condition is conducted. The model is based on the coupling of a three-dimensional (3D) co-rotational framework and a wake oscillator model, which includes axial, bending, and torsional degrees of freedom. These vary along the element length according to the discretization using Hermitian functions. The wake oscillator model is used to study vortex shedding, the drag and lift forces generated by the wake are described by the Van der Pol equations. The coupled equations are solved using the Newmark-β and Newton Raphson iterative scheme to obtain the VIV responses of the SCR. The VIV characteristics at different positions of the SCR are numerically simulated. The study explores the impact of current velocity on CF VIV. The results indicate that due to large deformations and flexible characteristics, the SCR predominantly vibrates at low frequencies, with the maximum vibration amplitude occurring in the transition segment, and multi-frequency resonance dominates the VIV response of the SCR, especially in the hung off segment.

Keywords: Steel catenary riser, Vortex-induced vibration, Wake oscillator model, Finite element method

1 Introduction

Steel Catenary Risers (SCRs) are essential transportation conduits that link seabed infrastructure to surface vessels in the oil and gas sector. They encounter multiple loads due to marine dynamics, such as hydrodynamic forces from waves and currents, internal flow impacts, and motions of the vessels[1].

Vortex-induced vibration (VIV) arises from the creation and shedding of vortices around a structure, resulting in oscillating forces and vibrations[2]. In contrast to top tension risers, the catenary form of a SCR introduces geometric nonlinearity and intricate 3D loads. Consequently, the three-dimensional VIV response of a SCR can substantially shorten the operational lifespan of the structure and compromise integrity of the system. Therefore, accurate prediction of VIV responses is crucial for the effective maintenance and safe operation of these facilities.

Given the lengthy calculation process involved in computational fluid dynamics (CFD) and the limitations of frequency domain methods in addressing nonlinearity[3], time-domain wake oscillator models are now favored for simulating VIV in offshore risers[4]. The Van der Pol wake oscillator is commonly used for predicting VIV in risers. It uses the acceleration interaction between the wake oscillator and structural motion. Studies have shown that the wake oscillator model can qualitatively capture the key VIV characteristics of risers. Skop and Balasubramanian [5] obtained quantitative agreement between the predictions of the diffusive van der Pol oscillator and experimental data in linearly shear flow. Facchinetti[6] demonstrated that the diffusive interaction along the continuously distributed van der Pol oscillators could model cellular vortex shedding in shear flow. Kurushina et al.[7] developed a new wake oscillator-based model in two dimensions to investigate VIV of a horizontal flexible structure with pinned-pinned ends in uniform flow. He et al.[8] used the generalized integral transform technique to study the vortex-induced vibration response of a fluid-conveying riser.

Although research on vortex-induced vibration is extensive in top tension risers, studies on the vortex-induced vibration of SCRs are still relatively limited. Yuan et al.[9] applied Euler-Bernoulli beam theory to investigate the

nonlinear seabed-riser interaction of an SCR considering the VIV response. Liu etal.[10] described the dynamics of flexible cylindrical bodies using the Euler-Bernoulli beam theory with absolute nodal coordinate formulation (ANCF) and studied the VIV response of SCRs using the finite element method. Li et al.[11] established a numerical model for calculating SCRs VIV and fatigue damage. The structural dynamics were accurately simulated using ANCF. Ma and Srinil[12] proposed an advanced numerical prediction model based on a nonlinear wake oscillator, utilizing the finite difference method to study the multi-directional VIV response of SCRs with structural bending.

This work conducts a numerical study on the cross-flow vortex-induced vibration of a steel catenary riser under uniform flow in three-dimensional large displacement conditions. The model is based on the coupling of a three-dimensional co-rotational framework and a wake oscillator model. The wake oscillator model is used to study vortex shedding, the drag and lift forces generated by the wake are described by the Van der Pol equations. The coupled equations are solved using the Newmark-β and Newton Raphson iterative scheme to obtain the VIV response of the SCR. Numerical simulations of the VIV characteristics at different positions of the SCR are conducted, exploring the impact of current velocity on the VIV of SCR.

2 Beam element of SCR

2.1 Reference configurations

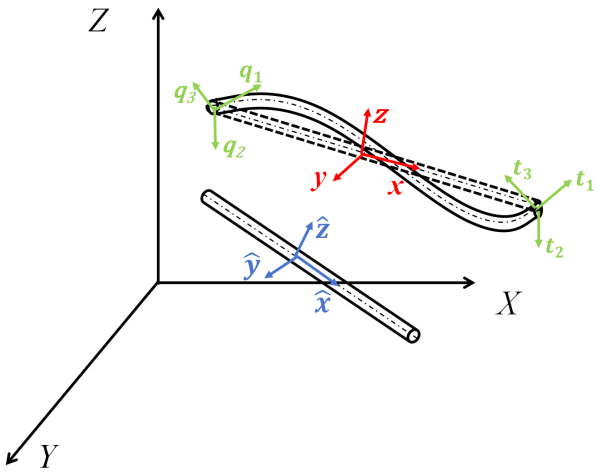

Figure 1. SCR element basic displaced frame in space.

The finite element method is employed based on the co-rotational formulation. It pertains to a linear space reference configuration, defined by the updated coordinates of two nodes. The assumption is that the element experiences large displacement and rotation, yet only minor strain. In this formulation, all variables reference a co-rotational configuration derived from the initial undeformed state via geometric transformations, such as rigid-body translations and rotations. This approach is commonly used in structural analysis, especially effective in dealing with large deformation problems.

In the co-rotational configuration method, we define three different states of configuration, as shown in Fig.1 The global system (*X, Y, Z*) serves as a spatial coordinate system that references the structure. The initial local element system ($\hat{x}, \hat{y}, \hat{z}$) corresponds to the undeformed configuration. The local element system (*x,y,z*) is associated with the reference configuration. In the co-rotational formulation, the element node systems (t_1, t_2, t_3), (q_1, q_2, q_3) are coordinate systems associated with each node.

2.2 Basic formulation for large rotations

In 3-D transformations involving a reference vector, Rodrigues' rotation formula[13] dictates the use of an orthogonal spatial transformation matrix $\mathbf{R}(\theta)$.

$$\mathbf{v}_1 = \mathbf{R}(\theta)\mathbf{v}_0 \tag{1}$$

In this case, the rotation matrix can be represented using quaternions,

$$\mathbf{R} = 2\begin{bmatrix} {q_0}^2 + q_1^2 - 1/2 & q_1q_2 - q_0q_3 & q_1q_3 + q_0q_2 \\ q_2q_1 + q_0q_3 & {q_0}^2 + {q_2}^2 - 1/2 & q_2q_3 - q_1q_0 \\ q_3q_1 - q_0q_2 & q_3q_2 + q_0q_1 & {q_0}^2 + {q_3}^2 - 1/2 \end{bmatrix} \tag{2}$$

where $\underline{\mathbf{q}}^T = \begin{bmatrix} q_0 & q_1 & q_2 & q_3 \end{bmatrix}$ are the so-called Euler parameters[14].

3 Fluid loads

In a riser system, the loads can be generated due to the flow of fluids both internally and externally. In this work, only the the buoyancy caused by the external fluid, fluid dynamics drag, and loads caused by vortex shedding are considered.

3.1 Fluid buoyancy

From the conditions of equilibrium, the equivalent nodal forces caused by the buoyancy of the external fluid are obtained[15]:

$$F_b^1 = 1/2\rho_w A_e l \quad \text{and} \quad F_b^2 = 1/2\rho_w A_e l \tag{3}$$

where F_b^1, F_b^2 are the equivalent nodal forces; ρ_w are the external fluid density; *l* is the element lenth; A_e are the external area.

3.2 Hydrodynamic forces

The structure is subjected to a uniform flow with a speed of $\mathbf{U}$ and density of ρ_{w}. The structure experiences fluid dynamic effects such as added mass, drag, and lift forces. We define the instantaneous relative velocity perceived by the riser $\mathbf{U}_{\text{rel}}$ based on $\mathbf{U}$ and the riser displacement $\mathbf{u}$ as: $\mathbf{U}_{\text{rel}} = \mathbf{U} - \dot{\mathbf{u}}$. In this model, the computation of fluid forces at every section and moment considers only the normal component of the flow velocity. The projection of relative velocity is denoted as $\mathbf{U}_{\mathrm{pr}}$. We define the vector $\mathbf{U}_{\mathrm{p}}$ as the projection of $\mathbf{U}$.

Added mass force

The added mass force per unit length is,

$$\mathbf{F}_a = m_{\mathrm{a}}(\dot{\mathbf{U}} - \ddot{\mathbf{u}}), \tag{4}$$

with $m_{\mathrm{a}} = C_a\rho_{\mathrm{f}}D^2\pi/4$ being the fluid added mass. The added mass coefficient C_a is assumed to be 1 [16] and $\dot{\mathbf{U}} = 0$.

Drag and lift forces

The drag and lift forces per unit length are:

$$\begin{aligned} \mathbf{F}_{\mathrm{drag}} &= \frac{1}{2}C_D\rho_w D\,|\mathbf{U}_{pr}|\,\mathbf{U}_{pr}, \\ \mathbf{F}_{\mathrm{lift}} &= \frac{1}{2}C_L\rho_w D\,|\mathbf{U}_{pr}|\,\mathbf{U}_{pr}\cdot\mathbf{R}. \end{aligned} \tag{5}$$

where $\mathbf{R}$ is a tensor of rotation, these forces are derived from experimental wake oscillator method, and drag and lift coefficients C_D and C_L. Ignoring the vortex-induced vibration in the inline direction, the lift coefficient is modeled by,

$$C_L = \frac{1}{2}C_{L0}q \tag{6}$$

where C_{L0} is the lift coefficient amplitude. The variable q is the dimensionless cross-flow wake variable. It can be seen as the normalized lift coefficient and [17]:

$$\ddot{q} + \epsilon\Omega_f \left(q^2 - 1\right)\dot{q} + \Omega_f^2 q = \frac{A}{D}\ddot{u}_q \tag{7}$$

where $\Omega_f = 2\pi S_t U \cos\phi / D$ is the vortex-shedding angular frequency, and St is the Strouhal number, ϵ and A are dimensionless parameters, $\ddot{u}_q$ is the cross-flow accelerations and defined as:

$$\ddot{u}_q = \ddot{\mathbf{u}} \cdot (\mathbf{e}_1 \times \mathbf{t}_{\mathrm{U}}) \tag{8}$$

with $\mathbf{t}_{\mathrm{U}}$ is the normalized projection of $\mathbf{U}$. $\mathbf{e_1}$ is the unit vector along the element axis.

The total hydrodynamic load results from the vector summation of Eqs.4 and 5, from which we can obtain the nodal equivalent hydrodynamics,

$$\mathbf{f}_h = \frac{1}{2}\mathbf{f}_h^1 + \frac{1}{2}\mathbf{f}_h^2 \tag{9}$$

where $\mathbf{f}_h^1$ and $\mathbf{f}_h^2$ are the forces at the two nodes of the element, respectively.

The distributed load from Eq.9 is transferred to the nodes using the element interpolation matrix,

$$\mathbf{F}_h = \int_0^\ell \mathbf{H}^T \mathbf{f}_h d\xi \tag{10}$$

where ξ represents the local coordinate along element axis, $\mathbf{F}_h$ is the nodal vector of hydrodynamic loads.

4 Finite element method

4.1 Element stiffness matrices

An appropriate formulation to compute elastic large displacement analysis, along with its consistent numerical implementation, is presented under Update and Total Lagrangian approaches. In the presence of large deflections, force equilibrium equations must be formulated for the deformed configuration. To accommodate geometric changes as external forces are applied, the solution to the nonlinear problem is linearized through a series of steps, each representing a load or time step. However, the presence of large deflections introduces nonlinear terms in strain-displacement equations, which are essential for calculating the stiffness matrix. Under a typical 3D nonlinear finite element approach the stiffness matrix is formed by linear contribution $\mathbf{K}_L$ gives by[18],

$$\mathbf{K}_L = \int_V \mathbf{B}_L^T \mathbf{C} \mathbf{B}_L dV \tag{11}$$

where $\mathbf{B}_L$ is the linear compatibility matrix, C is the elasticity matrix, and a non-linear geometric contribution $\mathbf{K}_G$ written as,

$$\mathbf{K}_G = \int_V \mathbf{B}_G^T \boldsymbol{\tau} \mathbf{B}_G \, dV \tag{12}$$

where $\mathbf{B}_G$ is the non-linear compatibility matrix, $\boldsymbol{\tau}$ is the stress matrix.

4.2 Element mass and damping matrices

$$\mathbf{M} = \int_V \rho_f \mathbf{H}^T \mathbf{H} dV, \quad \mathbf{D} = \int_V \kappa \mathbf{H}^T \mathbf{H} dV \tag{13}$$

where $\mathbf{M}$ is the mass matrix; $\mathbf{D}$ is the damping matrix; $\mathbf{H}$ is the interpolation matrix; ρ_f is the mass density for element; κ is the material damping parameter. In this paper, the structure damping is Rayleigh proportional damping.

4.3 Numerical implementation

The global dynamic equilibrium equation presented in matrix form as follows:

$$\mathbf{M}^{t+\Delta t}\ddot{\mathbf{u}} + \mathbf{D}^{t+\Delta t}\dot{\mathbf{u}} + {}^{t+\Delta t}\mathbf{K}\Delta\mathbf{u} = {}^{t+\Delta t}\mathbf{R} - {}^{t+\Delta t}\mathbf{F} \tag{14}$$

where $\Delta\mathbf{u}$ is the incremental displacements vector; ${}^{\mathbf{t}+\Delta t}\mathbf{R}$ is the global external force vector; and ${}^{t}\mathbf{F}$ is the structure internal forces vector at time t.

A step-by-step procedure has been implemented considering,

$$\begin{aligned} {}^{t+\Delta t}\ddot{\mathbf{u}} &= \frac{1}{\beta\Delta t^2}\Delta\mathbf{u} - \frac{1}{\beta\Delta t}{}^{t}\dot{\mathbf{u}} - \left(\frac{1}{2\beta} - 1\right){}^{t}\ddot{\mathbf{u}} \\ {}^{t+\Delta t}\dot{\mathbf{u}} &= {}^{t}\dot{\mathbf{u}} + (1-\gamma)\Delta t\,{}^{t}\ddot{\mathbf{u}} + \gamma\Delta t\,{}^{t+\Delta t}\ddot{\mathbf{u}} \\ {}^{t+\Delta t}\mathbf{u} &= {}^{t}\mathbf{u} + \Delta\mathbf{u} \end{aligned} \tag{15}$$

where β and γ are Newmark parameters.

5 Results and discussion

In order to model the simple SCR and start the dynamic analsis, an analytical approach presented by Faltinsen[19] was considered. The parameters of the SCR model and environment parameters are shown in Table.1. The empirical values in the wake oscillator equation are set as A = 12 and ϵ = 0.3, assuming C_D = 1.2, C_{L0} = 0.3, and St = 0.17. Figure.2 shows a schematic diagram of a SCR in uniform flow. Key points along the SCR, including the touchdown point (TDP) at node 200, transition point (TP) at node 1001, and hung off point (HOP) at node 2500, are selected for vibration response and frequency analysis.

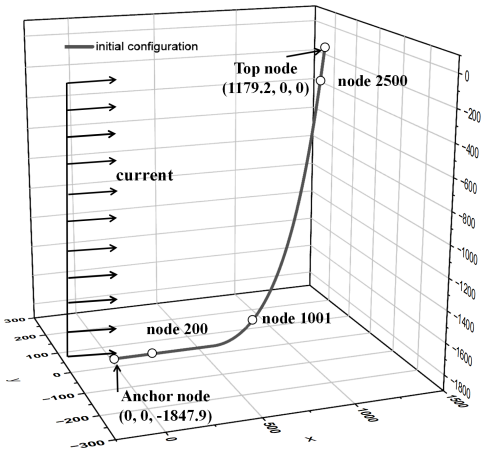

Figure 2. Initial configuration for the steel catenary riser under uniform flow.

Table 1. Parameters of the riser model and environmen

Parameters	Values
Riser Length: L (m)	2600
Outer diameter: D (m)	0.2032
Inner diameter: d (m)	0.165
Young's modulus: E (Pa)	2.06×10^{11}
Pipe density: ρ_s (kg/m^3)	7850
Sea water density: ρ_w (kg/m^3)	1024
Horizontal length(m)	1179.2
Water depth (m)	1847.9
Soil stiffness (N/m)	22500

Figures 3 to 5 show that the vibration displacement at the three positions of the SCR increases with the current velocity. The vibration amplitude of TP is greater than that of HOP and TDP, and the same is true for the frequency amplitude. The main frequency remains consistent across different current velocities. It is observed that the vibration response of the SCR in the CF direction is dominated by multiple frequencies. Notably, low frequencies dominate the displacement vibrations and correspond to larger amplitudes, especially in the hanging section.

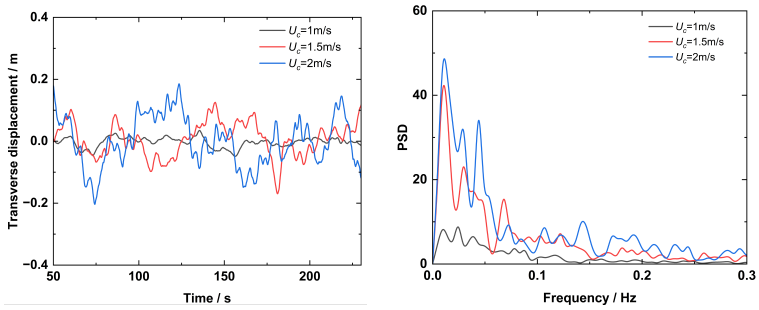

(a) (b)

Figure 3. Time history and spectrum of frequency of VIV displacement of the SCR in the CF direction at HOP under uniform flow with different velocities.

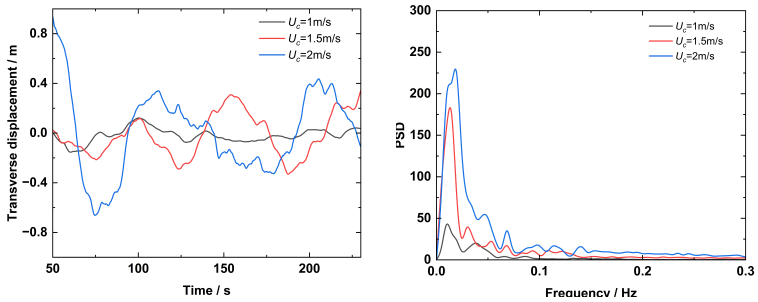

(a) (b)

Figure 4. Time history and spectrum of frequency of VIV displacement of the SCR in the CF direction at TP under uniform flow with different velocities.

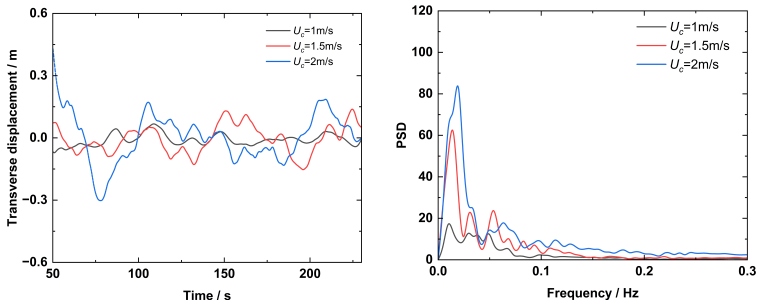

(a) (b)

Figure 5. Time history and spectrum of frequency of VIV displacement of the SCR in the CF direction at TDP under uniform flow with different velocities.

6 Conclusions

This study analyzes the cross-flow vortex-induced vibration response of a steel catenary riser under uniform flow. The fluid dynamics effects on the riser are represented using the Van der Pol wake oscillators. The complex interactions between the riser structure dynamics and ocean current were simulated using the finite element method and the Newmark integrator. Numerical results indicate that due to the large deformations and flexibility of the SCR, its vibrations are predominantly at low frequencies, with the maximum amplitude occurring in the transition section. The vortex-induced vibration response of the SCR is primarily characterized by multi-frequency resonance, especially in the hanging section. The study also emphasizes the necessity of considering large displacements and non-linearities in the modeling process. This research contributes to a deeper understanding of the challenges faced during the operation of offshore risers, particularly the impact of vortex-induced vibrations on the risers. This work can be extended to more realistic environments such as shear flow, conveying internal fluids.

Acknowledgements. The authors are grateful for the financial support provided by the Coordenação de Aperfeiçoamento de Pessoal de Nível Superior – Brasil (CAPES), Conselho Nacional de Desenvolvimento Científico e Tecnológico – Brasil (CNPq), FAPERJ, ANP, China National Petroleum Corporation (CNPC), and Embrapii.

Authorship statement. The authors hereby confirm that they are the sole liable persons responsible for the authorship of this work, and that all material included herein as part of this paper is either the property (and authorship) of the authors, or has the permission of the owners to be included here.

References

[1] C. An, M. Duan, S. F. Estefen, and J. Su. *Structural and Thermal Analyses of Deepwater Pipes*. Springer, 2021.

[2] A. Villié, M. C. Vanzulli, J. M. Zerpa, J. Vétel, S. Etienne, and F. P. Gosselin. Modeling vortex-induced vibrations of branched structures by coupling a 3d-corotational frame finite element formulation with wake-oscillators. *Journal of Fluids and Structures*, vol. 125, 2024.

[3] F. He, H. Dai, and L. Wang. Vortex-induced vibrations of a pipe subjected to unsynchronized support motions. *Journal of Marine Science and Technology (Japan)*, vol. 23, pp. 978–990, 2018.

[4] Y. Qu and A. V. Metrikine. A wake oscillator model with nonlinear coupling for the vortex-induced vibration of a rigid cylinder constrained to vibrate in the cross-flow direction. *Journal of Sound and Vibration*, vol. 469, 2020.

[5] R. A. Skop and S. Balasubramanian. A Nonlinear Oscillator Model For Vortex Shedding From A Forced Cylinder Part 2: Shear Flow And Axial Diffusion. *International Journal of Offshore and Polar Engineering*, vol. 5, n. 04, 1995.

[6] M. L. Facchinetti, E. deLangre, and F. Biolley. Vortex shedding modeling using diffusive van der pol oscillators. *Comptes Rendus Mécanique*, vol. 330, n. 7, pp. 451–456, 2002.

[7] V. Kurushina, E. Pavlovskaia, and M. Wiercigroch. Viv of flexible structures in 2d uniform flow. *International Journal of Engineering Science*, vol. 150, 2020.

[8] H. Y, of I. S. Offshore, and P. Engineers. *The proceedings of the Thirty-Third (2023) International Ocean and Polar Engineering Conference ISOPE-2023 : Ottawa, Canada, June 19-23, 2023*, 2023.

[9] Y. Yuan, M. Zheng, H. Xue, and W. Tang. Nonlinear riser-seabed interaction response among touchdown zone of a steel catenary riser in consideration of vortex-induced vibration. *Ocean Engineering*, vol. 227, 2021.

[10] D. Liu, S. Ai, L. Sun, and C. G. Soares. Vortex-induced vibrations of catenary risers in varied flow angles. *International Journal of Mechanical Sciences*, vol. 269, 2024.

[11] S. Li, C. Zhang, Z. Kang, and S. Ai. Effects of vertical and lateral riser-soil interactions on vortex-induced vibration of a steel catenary riser. *Ocean Engineering*, vol. 306, 2024.

[12] B. Ma and N. Srinil. Prediction model for multidirectional vortex-induced vibrations of catenary riser in convex/concave and perpendicular flows. *Journal of Fluids and Structures*, vol. 117, 2023.

[13] R. M. De Souza. *Force-based finite element for large displacement inelastic analysis of frames*. University of California, Berkeley, 2000.

[14] R. Magalhaes and D. Souza. Force-based finite element for large displacement inelastic analysis of frames, 2018.

[15] L. L. Aguiar, C. A. Almeida, and G. H. Paulino. Dynamic analysis of risers using a novel multilayered pipe beam element model, 2015.

[16] R. Blevins. *Flow-induced Vibration*. Krieger Publishing Company, 2001.

[17] Y. Gao, L. Liu, G. Pan, S. Fu, S. Chai, and C. Shi. Numerical prediction of vortex-induced vibrations of a long flexible riser with an axially varying tension based on a wake oscillator model. *Marine Structures*, vol. 85, 2022.

[18] K.-J. Bathet and S. Bolourchit. Large displacement analysis of three-dimensional beam structures, 1979.

[19] O. Faltinsen. *Sea loads on ships and offshore structures*, volume 1. Cambridge university press, 1993.